Available online at www.sciencedirect.com
ScienceDirect
Cement and Concrete Research 37 (2007) 258–263
Cement and Concrete Research

Young's modulus of cement paste at elevated temperatures

Joshua B. Odelson [1], Elizabeth A. Kerr [2], Wilasa Vichit-Vadakan *

CTLGroup, 5400 Old Orchard Road, Skokie, IL 60077, USA

Received 14 October 2005; accepted 1 November 2006

Abstract

Calcium silicate hydrate is a porous hydrate that is sensitive to temperature and readily loses strength at elevated temperatures. Mechanical and chemical changes in the microstructure, due to escaping water, can significantly affect the mechanical properties, but these changes occur over different temperature ranges. By measuring Young's modulus as a function of temperature using the dynamic mechanical analyzer, the temperature range in which the greatest change in stiffness occurs can be identified. Additional mineralogy, pore size distribution, and composition analysis from high temperature X-ray diffraction, nitrogen sorption, and thermogravimetric analysis will demonstrate the changes in the microstructure. The results demonstrate that over 90% of the loss in stiffness occurs below 120 °C. Therefore, the damage is due to microcracking caused by pore water expansion and evaporation and not the change in mineralogy or composition. More damage, as indicated by greater loss in stiffness, occurs in stiffer and less permeable samples where higher stresses can develop.

Keywords: Cement paste; Thermal analysis; Elastic moduli; Degradation; Temperature

1. Introduction

Although concrete has a well-deserved reputation for good fire resistance, it can lose 40–60% of its original strength upon exposure to 500 °C [1,2]. The most vulnerable yet also the most crucial component of concrete upon exposure to high temperature is the cement paste, the matrix of the composite. Cement paste is primarily composed of calcium silicate hydrate (CSH). This material naturally has high compressive strength but very low tensile strength. To improve these properties, concrete relies on the aggregate inclusions in the composite to increase the stiffness and the ductility while decreasing cost.

To achieve the ultimate goal of understanding the degradation mechanisms in concrete, the degradation mechanisms of each component must be understood. This paper focuses on the degradation of the cement paste alone, whose degradation mechanisms as it relates to mechanical properties are not well understood. Degradation mechanisms for cement paste upon exposure to high temperature include mechanical damage as well as chemical degradation; each mechanism is dominant within a specific temperature range, as described below. The Young's modulus can be used as a nondestructive indicator of damage incurred. Therefore, a study of the change in Young's modulus as a function of increasing temperature should yield results that indicate which mechanism causes the most damage.

Mechanical damage, in the form of microcracks alone, can cause significant strength degradation. Microcracking occurs because of two reasons. First of all, cement paste has extremely low permeability, even though the porosity can be quite high [3]. This is because the pore structure is very fine and possibly depercolated as the cement paste matures. Secondly, cement paste is naturally quite weak in tension so small increases in the volume of pore water, either simply due to expansion or to a phase change, can cause enough tensile stress in the cement paste to cause damage [4]. Unbound water expands and changes phases before evaporating from the porous body at about the

* Corresponding author. Tel.: +1 847 972 3072; fax: +1 847 965 6541.
E-mail address: WVichitVadakan@ctlgroup.com (W. Vichit-Vadakan).
[1] Present affiliation: Structural Engineer at DPR Construction, Redwood City, CA, USA.
[2] Present affiliation: Graduate Student in the Department of Civil Engineering Geological Sciences at University of Notre Dame, Notre Dame, IN 46556, USA.

0008-8846/$ - see front matter © 2006 Elsevier Ltd. All rights reserved.
doi:10.1016/j.cemconres.2006.11.006

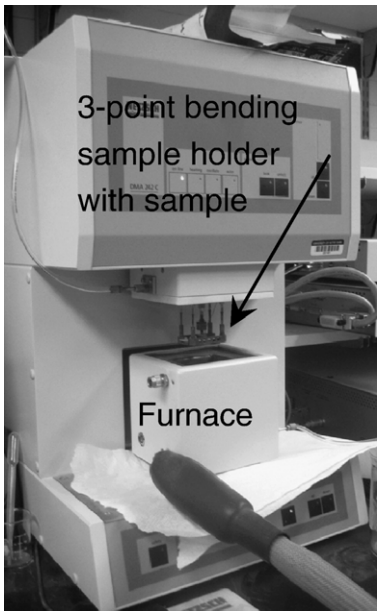

Fig. 1. Netzsch DMA 242 with the three-point bending fixture holding a cement paste plate ready to be tested.

boiling point of water, 100 °C. The combined effect of low tensile strength and low permeability in the cement paste can lead to significant mechanical damage at about the boiling point of water, especially where the cement paste happens to be saturated. Microcracking leads to increased permeability, decreased stiffness, and lower strength. If mechanical damage is the primary cause of loss in mechanical properties, then changes in such mechanical properties should be observed at about 100 °C.

There are two chemicals in cement paste that can degrade below 500 °C. CSH is typically reported to thermally decompose between 200 and 400 °C [5,6]. CSH thermally decomposes over a wide range of temperature because it is amorphous. Since CSH provides the primary load-bearing structure in hydrated cement, such decomposition would result in decreased stiffness and strength of the overall cement paste. In addition, calcium hydroxide (Portlandite) typically thermally decomposes at 580 °C [7]. Cement literature has reported Portlandite decomposition to occur as early as 425 °C [6,8]. Such decomposition would cause further damage to the remaining CSH because a drop in pH makes the CSH unstable. These chemical changes, either through the decomposition of CSH or Portlandite, can also degrade the stiffness and strength of the cement paste.

Although both mechanical and chemical degradation result in degradation of mechanical properties, the mechanisms occur at significantly different temperature ranges. A number of studies have been published on the changes in the microstructure of hydrated Portland cement, ranging from changes in the mineralogy to changes in pore structure [5,6,9–11]. In contrast, one paper has reported changes in the mechanical properties of cement paste, but such properties were reported as residual properties (properties measured after the sample has been heated and allowed to cool) vs. original properties (properties as measured before the sample is heated) [12]. Overall, there has been limited information on the mechanical properties of cement paste at elevated temperatures, and how changes in the mineralogy and composition directly affect the mechanical properties of the cement paste, which is the goal of this study.

Measurements of temperature dependent changes in stiffness are commonly done on plastics and metals through the use of a dynamic mechanical analyzer (DMA). The stiffness can be measured in compression or bending. Because of the stiffness and brittleness of cement paste, it is best to do such measurements in bending. In addition, the very thin samples required for bending (typically less than 2 mm) will minimize the temperature gradient within the sample. The DMA can be programmed to apply a displacement controlled cyclic load on the sample and calculate the change in stiffness based on known dimensions of the sample and the measured force. The three-point bending fixture is enclosed in a furnace for temperature control, as shown in Fig. 1, which allows the user to measure mechanical properties as a function of temperature. Through the use of the DMA, the most vulnerable temperature range can be identified by measuring the stiffness as a function of temperature. Changes in mineralogy and composition at elevated temperatures can be identified through the use of high-temperature X-ray diffraction (HTXRD) and thermogravimetric analysis (TGA). Such changes are important to be identified at the actual temperature, instead of being identified as residual properties. In addition, residual pore characteristics can be measured using nitrogen sorption. Although pore characteristics are difficult to measure at elevated temperatures, residual properties can give significant insight into the observed changes in the mechanical properties. The results of DMA, HTXRD, TGA, and nitrogen sorption experiments of cement paste samples with varying water–cement ratios (*w/c*)

Table 1
Mix design shown in kg of component per m^3 of cement paste

	Mix I	Mix II	Mix III	Mix IV	Mix V	Mix VII	Mix VIII	Mix X	Mix XI
Cement	1343	1177	1048	1379	1599	1392	1581	1386	1590
Water	536	589	629	460	392	465	387	463	389
Silica fume	0	0	0	153	0	0	175	77	88
Fly ash	0	0	0	0	177	154	0	77	88
w/c	0.40	0.50	0.60	0.33	0.24	0.33	0.24	0.33	0.24
w/B	0.40	0.50	0.60	0.30	0.22	0.30	0.22	0.30	0.22

Table 2
Specific gravities and BET surface areas

	Specific gravity (g/cc)	BET surface areas (m^2/g)
Type III cement	3.17	1.5391±0.0115
Silica fume	2.37	20.5486±0.3089
Fly ash	2.76	0.4812±0.0459

and loadings of fly ash and silica fume will be used to identify the dominant high temperature degradation mechanism of cement paste.

2. Method

Cement paste samples were prepared using Type III cement from LoneStar, Force 10,000 Microsilica from W.R. Grace, fly ash from the NIPSCO Plant in Wheatfield, IN, AdvaFlow high range water reducer from W.R. Grace, and deionized water. The specific gravities of the cement and mineral admixtures were measured using a Micromeritics Accupyc 1330 helium pycnometer.

Table 1 shows the mix designs for the different cement pastes. All samples were cast in 12 mm × 25 mm × 250 mm stainless steel molds. They were stripped from the molds at 24 h and cured in calcium hydroxide saturated water. These bars were trimmed to 1.5 mm × 10 mm × 55 mm plates using a Buehler Isomet 1000 diamond saw and continued to be stored in lime saturated water until the time of testing. This sample thickness was chosen to maximize measured displacement for the cement paste samples and to minimize temperature gradient during the experimental program. The sample width is prescribed by the DMA and the support span of the DMA fixture is 50 mm.

Between the ages of 90 and 100 days, the samples were tested under displacement-controlled oscillatory bending in a Netzsch Dynamic Mechanical Analyzer 242. During the test, the testing chamber was constantly purged with dry nitrogen. Samples were heated from room temperature to 400 °C under constant heating and a cooling rate of 2 °C/min with a constant temperature hold at 400 °C for 30 min. The maximum deflection is calculated such that the maximum stress on the sample is never greater than 2 MPa, to ensure that the sample does not undergo microcracking due to the loading. All measurements were done at 1 Hz. To ensure that stress corrosion was not causing the strength loss, companion samples were also tested at 0.5, 2, and 5 Hz.

Companion samples, directly from the saturated state, were crushed in a mortar and pestle and mixed with acetone for a smeared placement on a platinum plate. They were analyzed in a Bruker D8 Discovery Power Diffractometer with a Sol-X solid state detector that is equipped with a Bruker DHS900 Domed Heating Stage. Scans were taken at room temperature, 200 °C, and 550 °C.

Additional companion samples were also crushed and measured for decomposition temperatures in the Netzsch TG 209 thermogravimetric analyzer (TGA). The samples were exposed to ultra high purity dry nitrogen purge in the sample chamber to minimize any carbonation effects. The TGA samples underwent the identical thermal program as the DMA samples.

Finally, actual samples from DMA experiments were analyzed for pore characteristics using Micromeritics Accelerated Surface Area and Porosimetry Analyzer 2020. The samples were degassed under a vacuum until the vacuum stability was achieved and immediately analyzed. Samples not exposed to high temperatures were also analyzed for surface area. The samples were dried at room temperature in a vacuum dessicator prior to the surface analysis.

3. Results and discussion

The specific gravities and surface areas of the Type III cement, fly ash, and silica fume are reported in Table 2. This information was used to calculate the volumetric mix design of the cement paste samples.

Fig. 2 shows normalized modulus vs. temperature curves for cement paste with and without mineral admixtures. Because the different samples had different admixtures, the modulus ranged significantly. For ease in comparison, the in-situ results were normalized by the initial modulus measurement at room temperature, as measured at the start of the experiment when the sample was still saturated. Spikes in the modulus data occurred due to accidental contact between laboratory personnel and the table supporting the DMA. Four sets of data are presented in the plot. Mix IV, VII, and X have the same water/binder ratio but different admixture loadings, as shown in Table 1. Mix I is $w/c=0.4$ with no admixtures. The plot shows that the loss in modulus begins immediately as the sample begins to dry. This decrease slows down significantly by 200 °C. Beyond 200 °C, Young's modulus stays relatively constant. Although the magnitude of the loss in stiffness is different for each mix design, the temperature dependent pattern is consistent for all mix designs. Fig. 3 shows TGA results from companion samples. As expected, significant mass losses occur at about 100 °C where unbound water evaporates and between 200 and 350 °C where CSH decomposes. Companion samples were also analyzed using a HTXRD. The results indicated no chemical changes

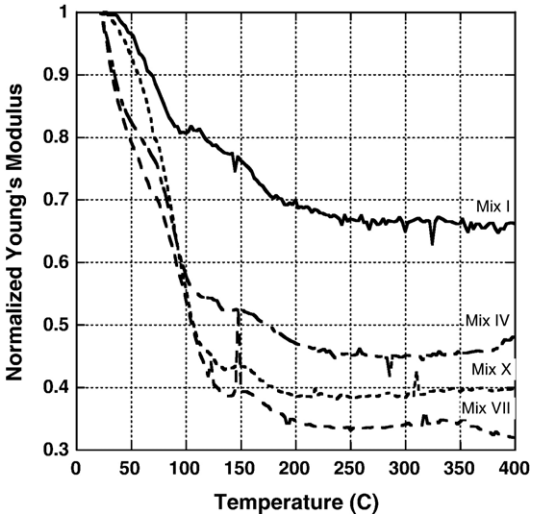

Fig. 2. Normalized modulus vs. temperature of cement paste with and without mineral admixtures.

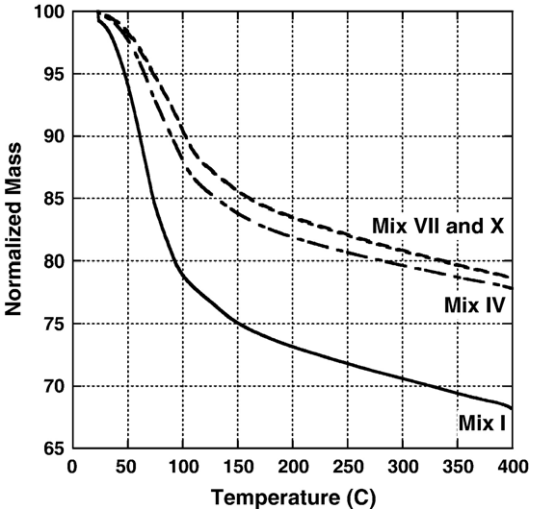

Fig. 3. Mass loss vs. temperature of cement paste with and without mineral admixtures.

below 100 °C, and significant chemical changes between 200 and 500 °C, which confirm the TGA results. The conclusion to combining the DMA data with the TGA and HTXRD data is that the primary damage mechanism for cement paste heated up to 400 °C is microcracking during the evaporation of unbound water since most of the damage occurred below 120 °C.

Another distinct indicator that the primary damage mechanism for cement paste exposed to high temperature is a process called pore coarsening. The exodus of water from the porous body causes significant cracking, increasing the average pore size, as shown in Table 3. Consistently, the average pore size, as calculated from the BJH desorption curve, was higher for the sample that had undergone high temperature exposure. It is interesting to note that the cumulative pore volume does not consistently increase also. This is likely due to the collapse of the interlayer surface area in CSH with the removal of pore water. Although further investigation of this behavior is needed, it extends beyond the scope of this study.

It is important not only to identify the damage mechanism, but to also identify the amount of decrease in Young's modulus. Fig. 4 shows the porosity as a function of the *w*/*B*. As expected, the porosity increased with increasing *w*/*B*. Fig. 5 shows the Young's modulus before any drying takes place, defined as the initial modulus. The initial modulus is plotted as a function of porosity. Again, as expected, the initial modulus decreased with increasing porosity. The modulus ranged from 14 to over 26 GPa. Fig. 6 is the companion plot to Fig. 5, showing the final modulus as a function of porosity. In this case, the final modulus ranged from 4 to 13 GPa, but the plot no longer demonstrates any correlation between the modulus and porosity, as shown in Fig. 5. Fig. 7 shows the residual Young's modulus normalized by the initial modulus, defined as normalized residual modulus, as a function of the initial modulus. The loss in modulus ranges from 35 to 75%. Finally, Fig. 8 shows the normalized residual modulus as a function of porosity. The cluster of three data points at the upper right quadrant of the plot are the results from the samples without mineral admixtures. These samples had higher *w*/*c* and no mineral admixtures. They consistently retained a higher percentage of the initial modulus, although the initial modulus was lower. The lower initial modulus likely allowed the sample to be more compliant, which resulted in lower tensile stresses and less overall damage during the evaporation of unbound water. The lower *w*/*B* samples, all of which contain mineral admixtures, consistently lost more than 50% of the initial modulus. Since the samples were tested at 90–100 days of age, it is expected that the mineral admixtures had sufficient time to react and refine the pores, causing decreased permeability. The combination of decreased permeability with increased stiffness yielded higher tensile stresses during the evaporation of unbound water and resulted in greater damage as indicated by greater loss in the modulus. Samples with 10% silica fume consistently yielded lower residual modulus, which demonstrates the pore refinement behavior, as silica fume has been shown to decrease the interfacial transition zone [13].

A concern with measuring modulus through oscillatory three-point bending is stress corrosion. The maximum allowable displacement is calculated such that the maximum tensile stress never exceeds 2 MPa, at the start of the experiment. The maximum amplitude of oscillation is fixed at that value throughout the experiment. Therefore, as Young's modulus decreases and the maximum strain is constant, the sample should not be damaged by the cyclic loads. To demonstrate that the loss in

Table 3
Pore characteristics as calculated by BJH using the desorption curve

Sample	Cumulative pore volume (cc/g)	Average pore size (Å)
Mix I — unheated	0.1878	60.2
Mix I — heated	0.1776	123.4
Mix IV — unheated	0.03584	76.2
Mix IV — heated	0.02875	201.5
Mix VII — unheated	0.03373	69.2
Mix VII — heated	0.03586	159.3
Mix X — unheated	0.03766	66.3
Mix X — heated	0.03492	173.1

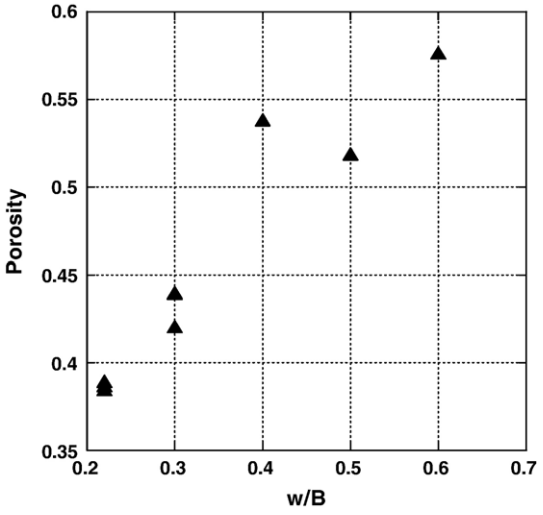

Fig. 4. Porosity vs. *w*/*B* of all mix designs.

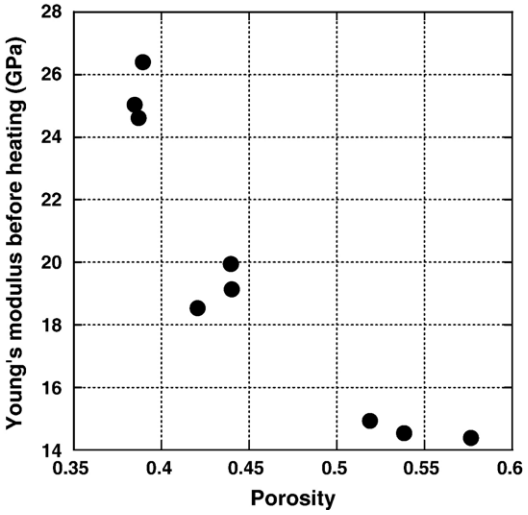

Fig. 5. Young's modulus as measured before heating vs. porosity.

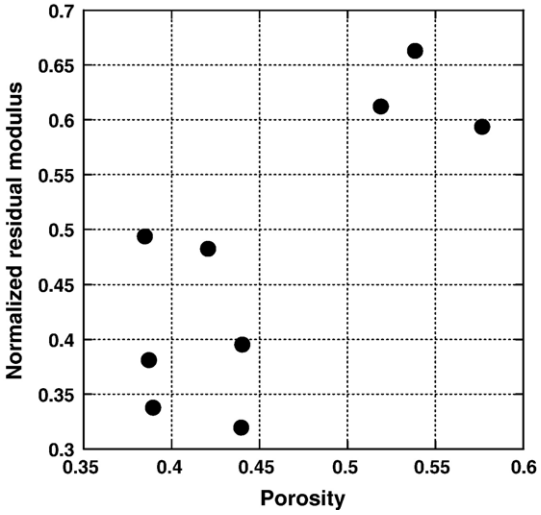

Fig. 8. Normalized residual modulus vs. porosity.

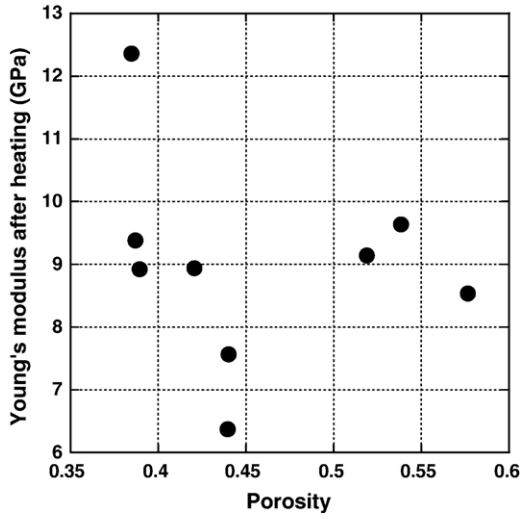

Fig. 6. Young's modulus as measured after heating vs. porosity.

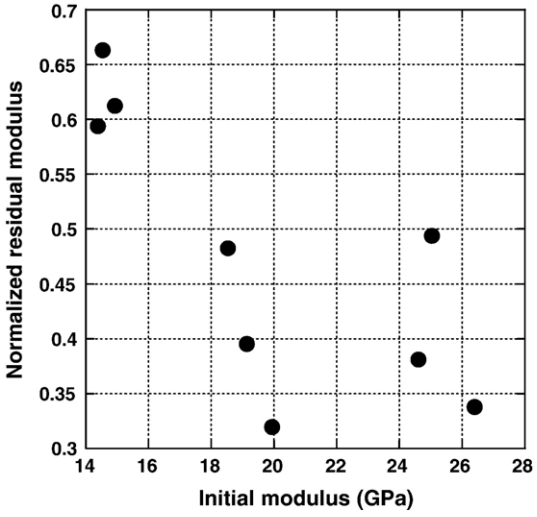

Fig. 7. Normalized residual modulus vs. Young's modulus as measured before heating.

Young's modulus is not due to stress corrosion, Fig. 9 shows companion samples from Mix X measured at three different frequencies. They all demonstrate the same behavior with losses in Young's modulus happening before 200 °C and consistent normalized residual modulus for all samples.

4. Conclusions

The experimental results consistently showed that the loss in stiffness for cement paste at elevated temperatures occurs predominantly below 120 °C, regardless of mix design. This indicates that the primary mechanism causing stiffness degradation is microcracking, which occurs as water expands and evaporates from the porous body. The loss in modulus due to chemical changes is insignificant after the sample is already microcracked. These results indicate that cement paste or concrete exposed to relatively low elevated temperatures of just 120 °C can develop significant damage. For small samples, the DMA has been

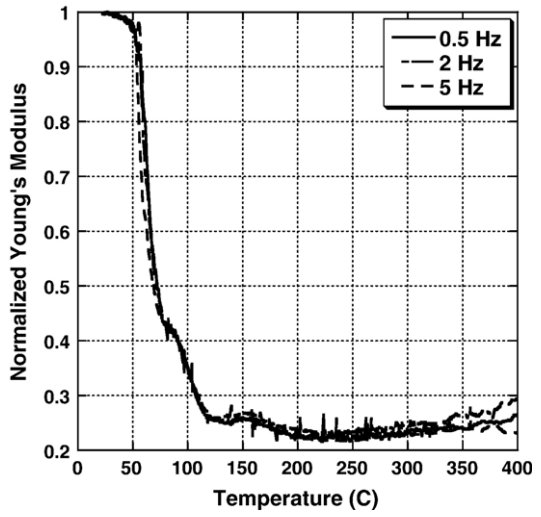

Fig. 9. Normalized Young's modulus as a function of temperature for companion Mix X samples measured under various oscillatory frequencies.

shown to be a useful tool to track changes in the mechanical properties with increasing temperature. The use of DMA data along with results from the TGA and HTXRD can provide significant insight into damage mechanisms of porous materials.

Acknowledgements

The work has been supported by a grant from the Henry Luce Foundation through the Clare Boothe Luce Program at the University of Notre Dame.

References

[1] A.H. Buchanan, Structural Design for Fire Safety, John Wiley and Sons, Chichester, West Sussex, 2002, p. 421.
[2] L.T. Phan, N.J. Carino, Mechanical properties of high-strength concrete at elevated temperatures, NISTIR 6726, National Institute of Standards and Technology, Gaithersburg, MD, 2001, p. 95.
[3] W. Vichit-Vadakan, G.W. Scherer, Measuring permeability of rigid materials by a beam-bending method: III. Cement paste, Journal of the American Ceramic Society 85 (6) (2002) 1537–1544.
[4] H. Ai, J.F. Young, G.W. Scherer, Thermal expansion kinetics: method to measure permeability of cementitious materials: II, application to hardened cement pastes, Journal of the American Ceramic Society 84 (2) (2001) 385–391.
[5] L. Alarcon-Ruiz, et al., The use of thermal analysis in assessing the effect of temperature on a cement paste, Cement and Concrete Research 35 (3) (2005) 609–613.
[6] C. Alonso, L. Fernandez, Dehydration and rehydration processes of cement paste exposed to high temperature environments, Journal of Materials Science 39 (9) (2004) 3015–3024.
[7] D.R. Lide (Ed.), CRC Handbook of Chemistry and Physics, 86th edition, Taylor and Francis, Boca Raton, 2004, p. 2544.
[8] H.F.W. Taylor, Cement Chemistry, Second edition, Thomas Telford, London, England, 1997, p. 459.
[9] I.A. Ibrahim, H.H. ElSersy, M.F. Abadir, The use of thermal analysis in the approximate determination of cement content in concrete, Journal of Thermal Analysis and Calorimetry 76 (3) (2004) 713–718.
[10] A. Moropoulou, A. Bakolas, K. Bisbikou, Characterization of ancient, byzantine and later historic mortars by thermal and X-ray diffraction techniques, Thermochimica Acta 269/270 (1995) 779–795.
[11] E.T. Stepkowska, et al., Thermo XRD-analysis of two aged cement pastes, Journal of Thermal Analysis and Calorimetry 80 (1) (2005) 193–199.
[12] S. Masse, et al., Elastic modulus changes in cementitious materials submitted to thermal treatments up to 1000 °C, Advances in Cement Research 14 (4) (2002) 169–177.
[13] J.M. Illston, P.L.J. Domone (Eds.), Construction Materials: their Nature and Behaviour, Spon Press, London, 2001, p. 554.